Effects of Ti doping on the structures and magnetic properties of $Fe_{16}N_2$ films

Effects of Ti doping on the structures and magnetic properties of $Fe_{16}N_2$ films

H Y Wang, E Y Jiang, D C Sun, H L Bai, P Wu and S L Ming

Department of Applied Physics, Tianjin University, Tianjin, 300072, People's Republic of China

Abstract. (Fe, Ti)–N films with the titanium concentration $C_{Ti} = 0$–35 at.% were prepared on Si(100) and NaCl substrates held at 150 °C by facing-target sputtering. The effects of Ti doping on the structures and magnetic properties of Fe–N films were investigated. The crystal structures of the (Fe, Ti)–N films were examined with an x-ray diffractometer and a transmission electron microscope. The formation of magnetic iron nitride phases is sensitive to the Ti doping concentration. Films with $C_{Ti} = 3$–10 at.% contain α''-$(Fe, Ti)_{16}N_2$ and $(Fe, Ti)_4N$ phases, and films with $C_{Ti} = 25$ at.% contain $(Fe, Ti)_4N$ and TiN phases, but there is no magnetic iron nitride phase in the films with $C_{Ti} = 35$ at.%. The saturation magnetization M_s of (Fe, Ti)–N films with $C_{Ti} = 0$–10 at.% was larger than that of pure bcc iron. M_s was 2.6 T for $C_{Ti} = 5$ at.% samples, which is higher than the value for pure iron by 17%.

1. Introduction

Over the past few years iron nitride has become a material system which has generated intense scientific interest because of the high magnetic moments that have been reported to range from 2.11 T [1] which is similar to that of bcc iron to the very impressive value of 2.9 T [2]. Among all of the magnetic phases present in Fe–N films, the α''-$Fe_{16}N_2$ phase is the most important because of its high magnetization value [3, 4]. However, no one has succeeded in obtaining $Fe_{16}N_2$ single-phase films. This is probably due to the fact that $Fe_{16}N_2$ exists only in a metastable ordered phase. Thus it is important to explore α''-alloy phases that might be more easily prepared and have better thermal stability than the pure α''-$Fe_{16}N_2$ phase. Almost all of the previous investigations have concentrated on pure bulk α''-materials and thin films; few papers have been published on the effects of the addition of a third element on the structures and magnetic properties of 16:2-type nitride.

In our previous work [5], we studied structures and magnetic properties of Fe–N films deposited by facing-target sputtering (FTS). In this study, we shall deal with (Fe, Ti)–N films and the effects of Ti doping on the structures and magnetic properties of Fe–N films in detail.

2. Experimental details

The (Fe, Ti)–N films were prepared by FTS on both Si(100) and NaCl substrates. The target used here was a pair of iron (99.99%) plates 100 mm in diameter. The sputtering gas and reactive gas were Ar (99.99%) and N_2 (99.99%) respectively. After the chamber was evacuated to a base pressure of 6×10^{-5} Pa, argon gas was introduced. During sputtering,

the Ar-gas pressure and N_2 pressure were kept constant at 3×10^{-1} Pa and $3\text{--}6 \times 10^{-2}$ Pa, respectively. The substrate temperatures were maintained at 150 °C. The composition of the (Fe, Ti)–N films was adjusted by varying the number of Ti chips mounted on iron targets. The deposition rate was about 0.25 nm s^{-1}.

The crystal structures of the (Fe, Ti)–N films were examined with an x-ray diffractometer (XRD) using Cu Kα radiation and a Hitachi H-9000 300 keV high-resolution transmission electron microscope capable of energy-dispersive x-ray (EDX) analysis. The magnetic properties were measured with a vibrating-sample magnetometer (VSM) in a magnetic field of 8 kOe at room temperature. The thickness of the film was measured by the multi-beam interference technique. The composition was also evaluated using XPS and electron probe analysis.
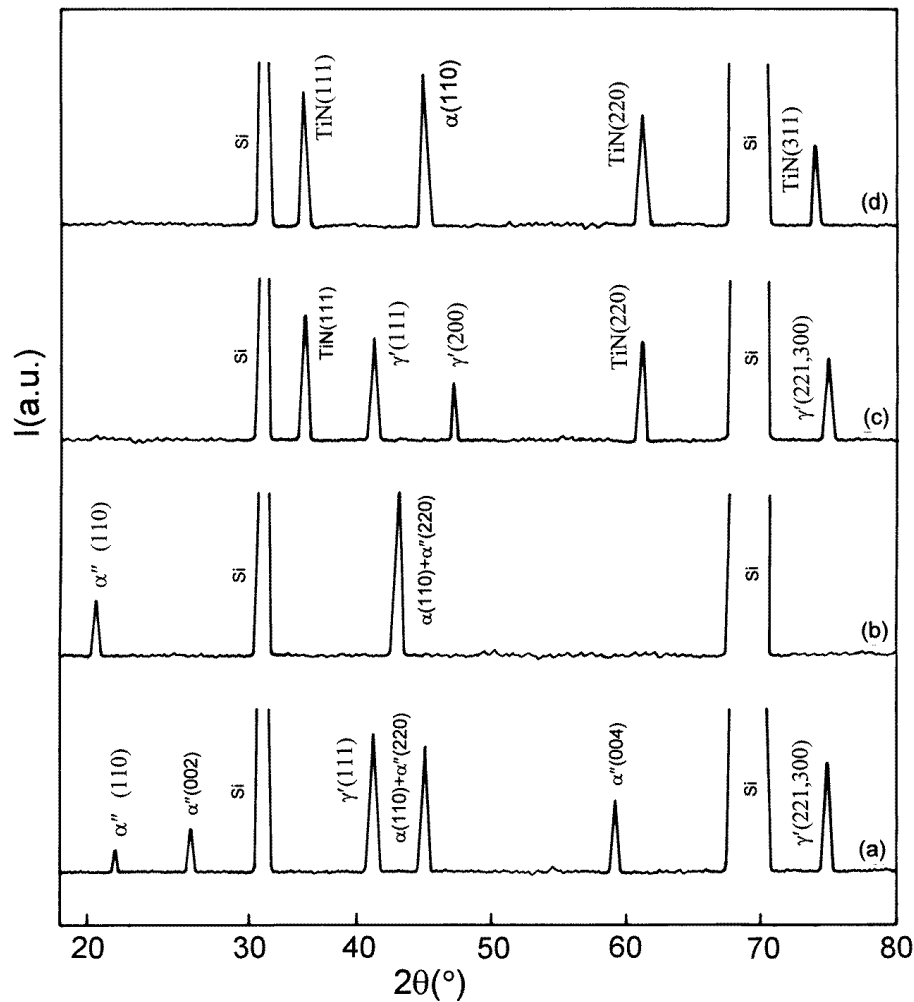

Figure 1. X-ray diffraction patterns of (Fe, Ti)–N films with various Ti concentrations: (a) $C_{Ti} = 0$ at.%; (b) $C_{Ti} = 5$ at.%; (c) $C_{Ti} = 25$ at.%; (d) $C_{Ti} = 35$ at.%.
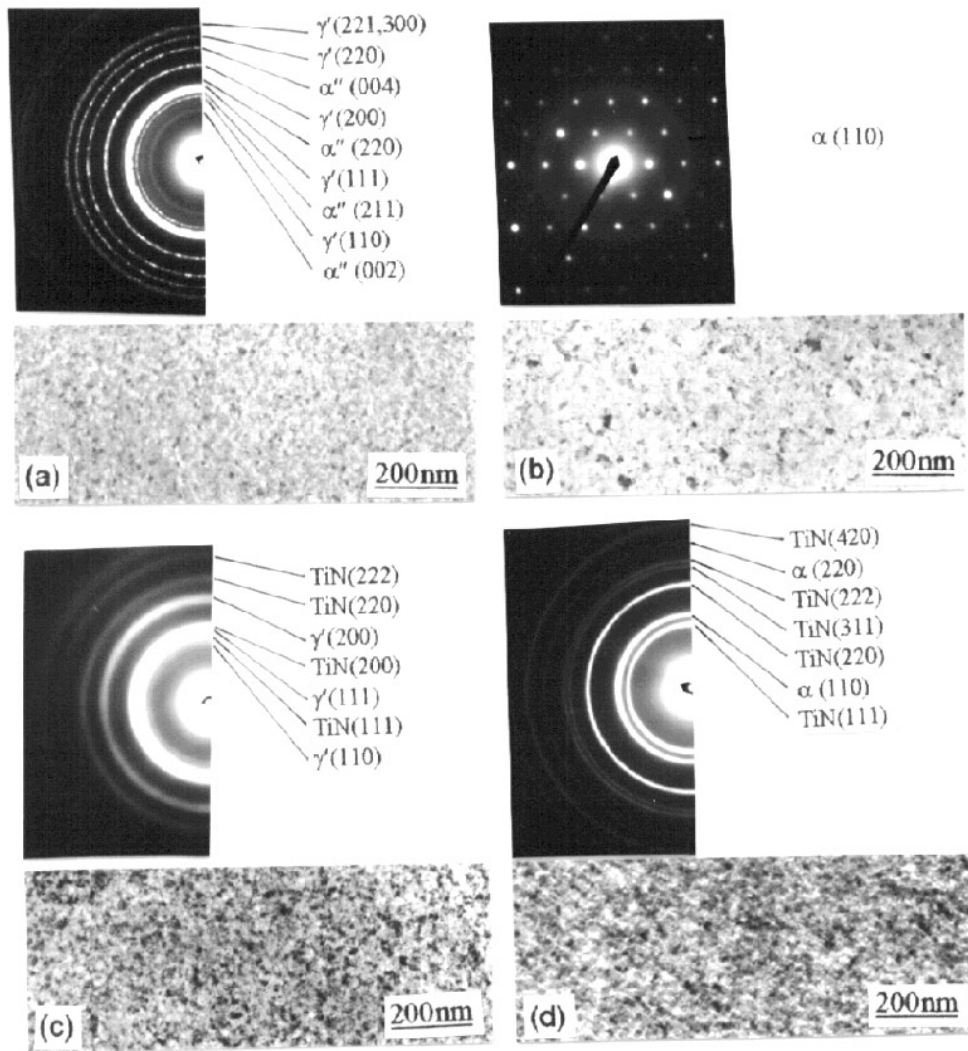
Figure 2. TEM bright-field images and SAD patterns of (Fe, Ti)–N films with various Ti concentrations corresponding to figures 1(a) to 1(d).

3. Results and discussion

Figure 1 shows the x-ray diffraction patterns of the (Fe, Ti)–N films with various titanium concentrations. In the titanium-free case, α''-$Fe_{16}N_2$(110), (002) and (004) peaks appear in the XRD, but the intensities of the α''-peaks are lower than those of the γ'-Fe_4N(111) and (221, 300) peaks, as shown in figure 1(a), showing that the volume fraction of α''-phase is less than that of the γ'-phase in the sample. Figure 1(b) shows the XRD of a 5 at.% Ti sample. A preferred grain orientation of the α''-phase is found in the sample. There is no evidence for Ti or Ti–N compounds in the XRD pattern. Ti atoms apparently dissolve substitutionally in the bcc Fe lattice. This illustrates why in the XRD patterns the positions of the α''(110) and (220) peaks of the 5 at.% Ti sample shift to low 2θ-values

(the lattice expands) compared with those of the titanium-free sample. In the XRD pattern of the 25 at.% Ti sample, the α''-phase disappears, but TiN and γ'-phases appear in the microstructure, as shown in figure 1(c). As the Ti content increases to 35 at.%, the 4:1 nitride peaks disappear, and only the peaks of TiN and Fe are observed, indicating that the formation of iron nitride is suppressed by the TiN phase for higher Ti contents.

Figure 2 shows the bright-field (BF) images and the selected-area diffraction (SAD) patterns corresponding to the specimens in figure 1. The indexing results are shown in figure 2. In figure 2(b), the SAD pattern consists of single-crystal diffraction spots and polycrystalline diffraction rings. The single-crystal spots are indexed as diffraction spots of the α''-phase along the $[\bar{1}11]$ direction in reciprocal space, and the polycrystalline diffraction ring is an α-Fe(110) ring. The intensity of the $\alpha(110)$ ring is lower than that of the single-crystal spots, showing that a large amount of preferentially oriented α''-phase formed in the sample. This agrees well with the XRD data shown in figure 1(b). An EDX analysis was made of the same area of the SAD pattern to determine the composition of the SAD area in the film. The composition of the area was determined to be: $C_{Fe} = 85$ at.%, $C_{Ti} = 5$ at.% and $C_N = 10$ at.%. There are no diffraction spots or rings of Ti or TiN compounds in the SAD patterns. Therefore the phase corresponding to the single-crystal spots in the SAD pattern was determined to be a Ti-containing 16:2 nitride, which can be denoted as α''-(Fe, Ti)$_{16}$N$_2$.
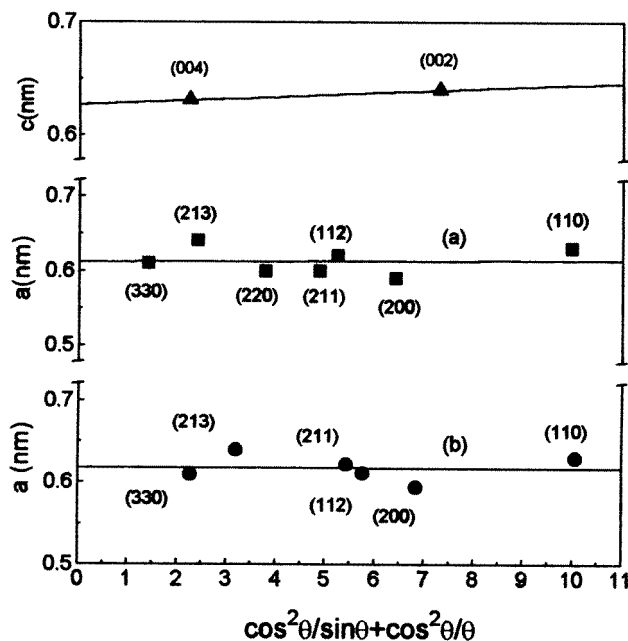

Figure 3. Extrapolation of the lattice constants a and c of the α''-phase against the Nelson–Riley function. (a) $C_{Ti} = 5$ at.%; (b) $C_{Ti} = 10$ at.%.

In order to determine accurate lattice constants a and c of the α''-(Fe, Ti)$_{16}$N$_2$ phase, the lattice constants a and c calculated from each plane are plotted against the Nelson–Riley function ($\cos^2 \theta / \sin \theta + \cos^2 \theta / \theta$) in figure 3. The extrapolated values of the lattice constants $a = 0.613 \pm 0.012$ nm and $c = 0.632 \pm 0.002$ nm for the α''-(Fe, Ti)$_{16}$N$_2$ phase are somewhat larger than those of the α''-Fe$_{16}$N$_2$ precipitates in bulk powder reported by
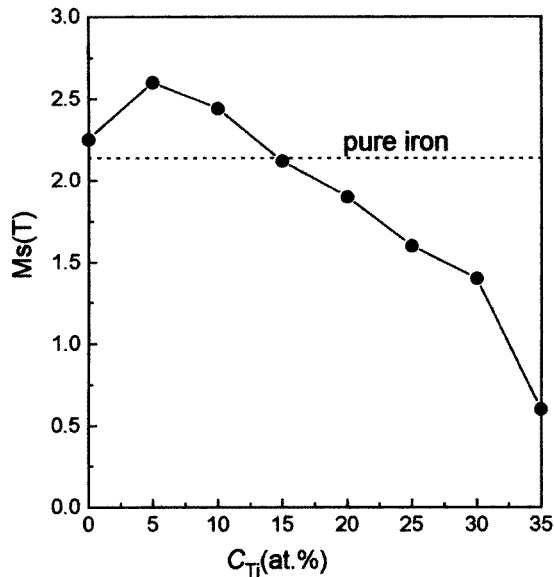
Figure 4. The dependence of the saturation magnetization M_s on the Ti doping content for (Fe, Ti)–N films.

Jack [6]. This difference indicates that the bct structure of the Ti-containing α''-phase was expanded along both the a- and c-axes, so the interstitial sites are wider in the Fe–Ti lattice than in the Fe lattice, suggesting that some Fe-atom positions are occupied by Ti atoms. The 16:2 nitride is considered to be a nitrogen-ordered form of the tetragonal Fe–N solid solution, which is derived without changing the basic arrangement of Fe atoms in the bcc structure. Therefore, it can be speculated that the Ti-containing 16:2 nitride also forms with less strain energy, leading to a higher stability, so a small Ti addition may benefit the α''-phase formation.

Figure 4 shows the dependence of the saturation magnetization M_s on Ti doping concentrations of (Fe, Ti)–N films. The value of M_s for films with $C_{Ti} = 0$–10 at.% is larger than that of pure iron. This is attributed to the contribution of the α''-phase in the films. For the $C_{Ti} = 5$ at.% film, it is $M_s = 2.6$ T, which is higher than that of pure iron by 17%. It is difficult to estimate quantitatively the volume ratio of α''-phase from the XRD pattern for the 5 at.% Ti film, because the peaks of $\alpha(110)$ and $\alpha''(220)$ overlap in the XRD pattern. Assuming a 25% volume fraction of α-Fe with $M_s = 2.1$ T and a 75% volume fraction of the α''-phase with $M_s = 2.8$ T, the calculated value is 2.62 T in good agreement with the measured value of 2.6 T. With the increase of the Ti content, M_s drops rapidly, because the films contain a large amount of TiN phase, as determined from XRD and TEM.

4. Conclusion

We have studied the effects of Ti doping on the structures and magnetic properties of α''-$Fe_{16}N_2$ films and found that the formation of magnetic iron nitride phases in (Fe, Ti)–N films is sensitive to the Ti doping content. When $C_{Ti} = 3$–10 at.%, it is advantageous to the formation of α''-$(Fe, Ti)_{16}N_2$ phase. The formation of magnetic iron nitride is suppressed by the presence of the TiN phase in the films with a higher Ti content. There is no magnetic

iron nitride phase in the films with $C_{Ti} = 35$ at.%. The saturation magnetization of (Fe, Ti)–N films with $C_{Ti} = 0$–10 at.% is larger than that of pure bcc iron. The average saturation magnetization value is 2.6 T for the $C_{Ti} = 5$ at.% sample, which is higher than that of pure iron by 17%. It is suggested that appropriate Ti doping might stabilize the 16:2 nitride structure.

Acknowledgments

References

[1] Takahashi M, Shoki H, Takahashi H and Wakiyama M 1993 *IEEE Trans. Magn.* **29** 102
[2] Komuro M, Kozono Y, Hanazono M and Sugita Y 1990 *J. Appl. Phys.* **67** 5126
[3] Sugita Y, Mitsuoka K, Komuro M, Hoshiya H, Kozono Y and Hanazono M 1991 *J. Appl. Phys.* **70** 5977
[4] Takahashi H, Mitsuoka K, Komuro M and Sugita Y 1993 *J. Appl. Phys.* **73** 6060
[5] Jiang E Y, Sun C Q, Li J and Liu Y G 1989 *J. Appl. Phys.* **65** 1659
[6] Jack K H 1951 *Proc. R. Soc.* A **208** 216